

ω - and ϕ -meson production in $pn \rightarrow dV$ reactions and OZI-rule violation

L.A. Kondratyuk^{a,1}, Ye.S. Golubeva^{b,1} and M. Büscher^{c,1}

^a*Institute of Theoretical and Experimental physics, B. Chermushkinskaya 25, 117259 Moscow, Russia*

^b*Institute for Nuclear Research, 60th October Anniversary Prospect 7A, 117312 Moscow, Russia*

^c*Forschungszentrum Jülich, Institut für Kernphysik, 52425 Jülich, Germany*

Abstract

We investigate the reactions $pn \rightarrow d\omega$ and $pn \rightarrow d\phi$ close to threshold and at higher energies. Near threshold we calculate the S -wave amplitudes within the framework of the two-step model which is described by a triangle graph with π -mesons in the intermediate state and find a ratio of the S -wave amplitudes squared of $R = |A_\phi|^2/|A_\omega|^2 = (4-8) \times 10^{-3}$. Any significant enhancement of the experimental value of $R(\phi/\omega)$ over this prediction can be interpreted as a possible contribution of the intrinsic $s\bar{s}$ component in the nucleon-wave function. We present arguments that there is a strong resonance effect in the ωN channel close to threshold. At higher energies we calculate the differential cross sections of the reactions $pn \rightarrow d\omega$, $pn \rightarrow d\phi$ and the ratio of the ϕ/ω yields within the framework of the quark-gluon string model. An irregular behavior of the ϕ/ω -ratio is found at $s \leq 12 \text{ GeV}^2$ due to the interference of the t - and u -channel contributions.

PACS 25.10.+s; 13.75.-n

Key words: Meson production; Omega; Phi; OZI rule; pn.

1 Introduction

It is well known (see e.g. [1-3]) that the ratio of the ϕ/ω yields

$$R = \frac{\sigma_{A+B \rightarrow \phi X}}{\sigma_{A+B \rightarrow \omega X}}, \quad (1)$$

¹ Supported by DFG and RFFI.

where the initial and final hadrons do not contain strange quarks, is a particularly sensitive probe of the OZI rule [4]. At the standard deviation $\delta = \theta - \theta_1 = 0.7^\circ$ from the ideal $SU(3)_f$ mixing angle $\theta_1 = 35.3^\circ$ we have $R/f = 4.2 \times 10^{-3}$ [3], where f is the ratio of the phase-space factors. However, experimental data show an apparent excess of R/f above the standard value which varies from $(10 - 30) \times 10^{-3}$ in πN and NN collisions to $(100 - 250) \times 10^{-3}$ in $\bar{N}N$ annihilation at rest and in flight (see e.g. the discussion in [3]). In [3] the big excess of R in pp and $\bar{p}p$ collisions over the prediction by the OZI rule was treated in terms of “shake-out” and “rearrangement” of an intrinsic $\bar{s}s$ component in the nucleon wave function. On the other hand, in papers [5,6] the strong violation of the OZI rule in $\bar{p}p$ annihilation at rest was explained in terms of hadronic intermediate $K\bar{K}^*$ states which might create ϕ mesons.

Another argument in favour of a large admixture of hidden strangeness in nucleons was related to an apparently large contribution of the ϕ -meson into the isoscalar spectral function which through the dispersion relation defines the isoscalar nucleon form factor (see Ref.[7]). However, as it was shown later (see [8] and references therein), the main contribution to the isoscalar spectral function near 1 GeV stems from correlated $\pi\rho$ exchange which does not involve strange quarks.

Therefore, the question whether there is a large admixture of hidden strangeness in nucleons seems to be unclarified. Thus, it is important to investigate such reactions where uncertainties in the interpretation of ω and ϕ production in terms of intermediate hadronic states would be comparably small. In this paper we argue that a good choice in this respect is the reaction

$$pn \rightarrow dV , \quad (2)$$

where V denotes the vector mesons ω and ϕ .

We show that contributions of the hadronic intermediate states into the S -wave amplitudes of the reactions $pn \rightarrow d\phi$ and $pn \rightarrow d\omega$ can be predicted rather reliably using the two-step model described by triangle graphs with π mesons in the intermediate state [9,10]. Therefore, if the ϕ and ω yields will be measured in reaction (2) near threshold (which e.g. can be done at COSY-Jülich), the results can be useful for a better understanding of the OZI-rule violation dynamics. For example, any essential deviation from the prediction of the two-step model could be serious evidence for the above mentioned “shake out” or “rearrangement” of an intrinsic $\bar{s}s$ component in the nucleon wave function.

Note that recent measurements of the ϕ/ω ratio in the reaction $pd \rightarrow {}^3HeX$ (performed at SATURNE II [11,12]) yield

$$R/f = \left(63 \pm 5 \begin{smallmatrix} +27 \\ -8 \end{smallmatrix}\right) \times 10^{-3} \quad (3)$$

which is also clearly above the expectation 4.2×10^{-3} . However the dynamics of the reaction $pd \rightarrow {}^3HeX$ is not yet understood. According to [13] the two-step model underestimates the SATURNE data by a factor 2, while according to [14] the discrepancy of the two-step model with the data might be even larger when spin-effects are taken into account.

Experiments on ω and ϕ production in the reaction $pp \rightarrow ppV$ close to threshold were performed by the SPES3 and DISTO collaborations at SATURNE (Saclay) [15,16] (see also the calculations of ω production in [17]). Near threshold the dynamics of the reactions $pp \rightarrow ppV$, $pn \rightarrow pnV$ and $pn \rightarrow dV$ are different because the first one is constrained by the Pauli principle and the two protons in the final state should be in a 1S_0 state. In the third case the final pn system is in the 3S_1 state while in the second case it can be in both states. Therefore, a possible violation of the OZI rule is expected to be different in all those cases.

Another interesting point is that within the framework of the line-reverse invariance (LRI) assumption the reaction $pn \rightarrow dV$ can be related to the Pontecorvo reaction $\bar{p}d \rightarrow VN$. The data from the OBELIX and Crystal-Barrel collaborations result in a ϕ/ω ratio of about $(230 \pm 60) \times 10^{-3}$ [18]. Therefore, if LRI is applicable we expect the violation of the OZI rule in the reaction $pn \rightarrow dV$ to be much larger than it is predicted by the two-step model, which assumes the dominance of the hadronic intermediate states.

We also consider reaction (2) at higher energies, analyzing it in terms of Kaidalov's quark-gluon string model [19]. Within the framework of this model the amplitude of reaction (2) is dominated by three valence-quark exchange in the t - and u -channels. This mechanism corresponds to the nucleon Regge-pole exchange and reaction (2) can be related to other reactions like πN backward scattering and reactions $pp \rightarrow d\pi^+$, $\bar{p}d \rightarrow p\pi^-$. Therefore, the parameters describing the Regge trajectory and the t -dependence of residues can be taken from other experimental data except for the overall normalization. The latter can be fixed using the prediction of the two-step model at lower energy. In this way we can predict the differential cross sections of the reactions $pn \rightarrow d\phi$, $pn \rightarrow d\omega$ and $R(\phi/\omega)$ in wide intervals of energy and momentum transfer.

The paper is organized as follows. In Sect.2 we analyze the reactions $pn \rightarrow d\phi$ and $pn \rightarrow d\omega$ near the thresholds within the framework of the two-step model. In Sect.3 we consider the quark-gluon string model. In Sect.4 we present our conclusions.

2 The non-relativistic two-step model

Let us in the beginning consider the time-reversed reaction

$$Vd \rightarrow pn \quad (4)$$

where V is the vector meson, ω or ϕ . In order to avoid complications related to the Lorentz-boost of the bound system it is convenient to calculate the amplitude of reaction (4) in the deuteron rest frame. Reaction (4) is very similar to the Pontecorvo reaction of meson production in $\bar{p}d$ annihilation

$$\bar{p}d \rightarrow MN . \quad (5)$$

The branching ratios for reaction (5) with $M = \pi, \eta, \eta', \rho, \omega$ and ϕ were described in [10] within the framework of the two-step model (TSM). The results are presented in Table 1, where it is seen that the model reproduces BR's for vector meson production rather well. Here we shall use the TSM for the description of reaction (4). In the TSM, which can be described by the diagrams in Fig.1, reaction (4) proceeds in two steps: (i) in the first step the vector meson V creates a π meson on one nucleon through the reaction $\omega N \rightarrow N\pi$ and (ii) in the second step the π meson is absorbed by the other nucleon.

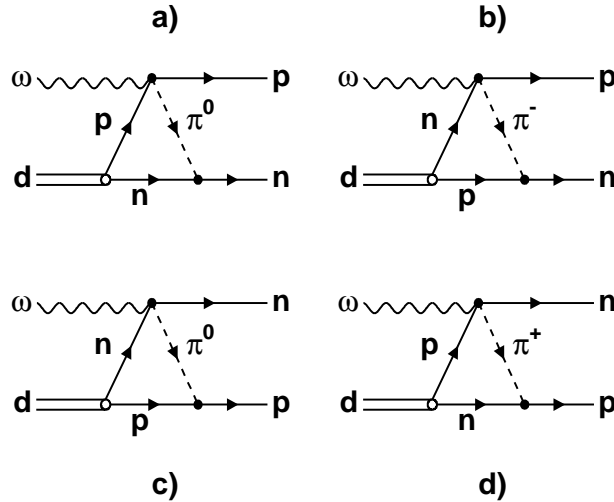


Fig. 1. Diagrams describing the two step model for the case $V = \omega$.

First we investigate reaction (4) at small momenta of the ω meson when only the S waves in the VN and Vd systems contribute significantly. Then the amplitude of the reaction

$$VN \rightarrow N\pi \quad (6)$$

can be written as

$$\langle p'_3; p'_4 \lambda'_n | \hat{T}_{VN \rightarrow N\pi} | p'_1, \vec{\epsilon}_{\lambda'_1}^{(V)} p'_2 \lambda'_2 \rangle = \varphi_{\lambda'_4}^*(\vec{p}'_4) \vec{\epsilon}_{\lambda'_1}^{(V)} \cdot \vec{\sigma} \varphi_{\lambda'_2}^*(\vec{p}'_2) A_{VN \rightarrow N\pi}(s_1, t_1), \quad (7)$$

where p'_1, p'_2, p'_3 and p'_4 are the 4-momenta of the vector meson, the initial nucleon, the final nucleon and the π meson, respectively. The λ'_i are the spin projections and the $\vec{\epsilon}^{(V)}$ is the polarization vector of the vector meson and $s_1 = (p'_1 + p'_2)^2 = (p'_3 + p'_4)^2$, $t_1 = (p'_1 - p'_4)^2 = (p'_2 - p'_3)^2$. The amplitude of reaction (4) which corresponds to the triangle graph of Fig.1 has the following form:

$$T_{Vd \rightarrow pn}(s, t) = \frac{f_\pi}{m_\pi} \varphi^*(\vec{p}_4) \vec{\sigma} \cdot \vec{\epsilon}^{(d)} \vec{\sigma} \cdot \vec{\epsilon}^{(V)} \vec{\sigma} \cdot \vec{M}^{(\pi)} \varphi(\vec{p}_3) \cdot A_{VN \rightarrow N\pi}(s_1, t_1), \quad (8)$$

where

$$M_i^{(\pi)} = \sqrt{2m} \int q_i \Phi_\pi(\vec{k}, \vec{p}_4) \Psi_d(\vec{k}) \frac{d^3k}{(2\pi)^{3/2}} \quad (9)$$

$$\Phi_\pi(\vec{k}, \vec{p}) = \frac{F_1(q^2) F_2(q^2)}{q^2 - m_\pi^2} \quad (10)$$

$$q^2 = m_\pi^2 - \delta_0(\vec{k}^2 + \vec{p} \cdot \vec{k} + \beta(\vec{p}_4)),$$

$$\vec{p} = -2\vec{p}_4/\delta_0, \quad \vec{q} = \vec{p}_4 - \vec{k},$$

$$\beta(\vec{p}_4) = (\vec{p}_4^2 + m_\pi^2 - T_4^2)/\delta_0,$$

$$\delta_0 = 1 + T_4/m.$$

Here, p'_1, p'_2, p'_3 and p'_4 are the 4-momenta of the vector meson, deuteron, proton and neutron, respectively, and $s = (p_1 + p_2)^2$, $t = (p_1 - p_3)^2$, $u = (p_1 - p_4)^2$. $T_4 = E_4 - m$ is the proton kinetic energy, $\Psi_d(\vec{k})$ the deuteron wave function, $\vec{\epsilon}^{(d)}$ is the polarization vector of the deuteron, $f_\pi \approx 1$ is the πNN coupling constant, $F_1(q^2)$ is the form factor in the πNN vertex, $F_2(q^2)$ is the form factor which cuts virtual masses of the π meson in the amplitude $\omega N \rightarrow N\pi$. Note that the amplitude $M_i^{(\pi)}$ corresponds to the exchange of the neutral π meson (see the left diagrams in Fig.1).

Apart from the π exchange some contributions to the $Vd \rightarrow pn$ amplitude might also come from other exchanges like ρ or ω mesons. As it was shown in [10], ρ or ω exchanges give only small contributions to the amplitudes of the Pontecorvo reactions $\bar{p}d \rightarrow MN$. This can be seen in Table 1 taken from [10].

The rather strong suppression of those exchanges is related to the fact that they are mainly contributing at smaller internucleon distances as compared to

Table 1

Contributions of different intermediate channels into BR's for different Pontecorvo reactions ($\times 10^{-6}$) within the framework of TSM. The experimental data are taken from [20,21].

| $\bar{p}d \rightarrow MN$ | Intermediate state | Contribution only S -wave | Contribution S and D wave | Experiment |
|---------------------------|--------------------|-----------------------------|-------------------------------|-----------------|
| π^-p | π | 12.69 | 12.89 | 12.9 ± 0.8 |
| | ρ | 0.12 | 0.09 | |
| | ω | 0.02 | 0.01 | |
| | Total | 12.8 ± 0.4 | 12.9 ± 0.5 | |
| ηn | π | 1.3 | 1.34 | 3.19 ± 0.48 |
| | ρ | 0.2 | 0.18 | |
| | ω | 0.03 | 0.03 | |
| | Total | 1.6 ± 0.2 | 1.6 ± 0.2 | |
| $\eta'n$ | π | 2.03 | 2.03 | 8.2 ± 3.4 |
| | ρ | 0.25 | 0.25 | |
| | ω | 0.05 | 0.05 | |
| | Total | 2.3 ± 0.2 | 2.3 ± 0.2 | |
| ρ^-p | π | 17.86 | 17.91 | 29.0 ± 7.0 |
| | ρ | 0.33 | 0.29 | |
| | ω | 0.06 | 0.06 | |
| | Total | 18.3 ± 2.3 | 18.3 ± 2.3 | |
| ωn | π | 28.35 | 28.41 | 22.8 ± 4.1 |
| | ρ | 0.73 | 0.66 | |
| | ω | 0.06 | 0.05 | |
| | Total | 29.1 ± 1.7 | 29.1 ± 1.7 | |
| ϕn | π | 5.54 | 5.54 | 5.3 ± 0.9 |
| | ρ | 0.03 | 0.03 | |
| | ω | 0.003 | 0.003 | |
| | Total | 5.6 ± 0.7 | 5.6 ± 0.7 | |

π exchange. We checked that the contributions of ρ and ω exchanges can also be neglected in the reactions considered here.

It was shown in [10] that the deuteron D -wave contribution into the amplitudes of Pontecorvo reactions is very small as compared to the S -wave (see Table 1). Therefore, here we take into account only the S -wave in the deuteron wave function. As in [10] we use the Paris model for the description of the deuteron wave function, parameterized as in [22].

The product of the two form factors in Eq.(10) we parameterize using the dipole formula

$$F_1(q^2)F_2(q^2) = \left(\frac{m_\pi^2 - \Lambda^2}{q^2 - \Lambda^2} \right)^2 . \quad (11)$$

The best description of the data on Pontecorvo reactions was found with $\Lambda = 1.1$ GeV [10] and here we choose the cut-off parameter in the interval $1.0 - 1.2$ GeV/c.

At small momenta of the vector meson the differential cross section is isotropic in the CM system and the amplitude $A_V(s_1, t_1)$ can be expressed through the total cross section of the reaction $\pi^- p \rightarrow Vn$ as follows

$$|A_{VN \rightarrow N\pi}(s_1, t_1)|^2 = \frac{16 \pi s_1}{3} \frac{k_\pi^{\text{cm}}(s_1)}{k_V^{\text{cm}}(s_1)} \sigma(\pi^- p \rightarrow Vn) . \quad (12)$$

For the cross section $\pi^- p \rightarrow n\omega$ we use two different parameterizations from [23] and [24] which well reproduce the available experimental data. For the cross section $\pi^- p \rightarrow n\phi$ we take the fit from [24]. Note that very close to threshold ($k_V^{\text{cm}}(s_1) \leq 100 - 120$ MeV/c) the S -wave amplitude of the reaction $\pi^- p \rightarrow n\omega$ is suppressed (see [25]). In the case of the reaction $\pi^- p \rightarrow n\phi$ there is also some indication that $\sigma/k_V^{\text{cm}}(s_1)$ has an irregular behavior at very small $k_V^{\text{cm}}(s_1)$. As the origin of this effect is not completely clear we shall use the TSM for calculation of the cross sections of the reactions $Vd \rightarrow pn$ and $pn \rightarrow Vd$ at those values of s which correspond to $k_V^{\text{cm}}(s_1)$ larger than 150 MeV/c. The experimental data show that the angular distribution in the reaction $\pi^- p \rightarrow n\omega$ is isotropic and the S -wave is dominant at least until $k_V^{\text{cm}}(s_1) = 260$ MeV/c (see the comment on p.2805 in [25]). So we shall use the TSM model in the energy region which corresponds to $k_V^{\text{cm}}(s_1) = 150 - 260$ MeV/c. At other energies we use the predictions of the QGSM, normalized to the TSM model at an energy corresponding to $k_V^{\text{cm}}(s_1) \simeq 200$ MeV/c.

The differential cross section of reaction (4) can be written as

$$\frac{d\sigma_{Vd \rightarrow pn}}{dt} =$$

$$\frac{1}{64 \pi s} \frac{1}{(p_{\omega}^{\text{cm}})^2} F(I) \overline{|T_{Vd \rightarrow pn}(s, t) + T_{Vd \rightarrow pn}(s, u)|^2}. \quad (13)$$

The isospin factor $F(I)$ in Eq.(13) takes into account the exchange of π^0 and π^- in the intermediate state and is defined as

$$\begin{aligned} |T^{(a)} + T^{(b)}|^2 &= F(I) |T^{(a)}|^2 \\ |T^{(c)} + T^{(d)}|^2 &= F(I) |T^{(c)}|^2 \end{aligned}$$

and is equal to 9. The indices (a) to (d) correspond to the four diagrams in Fig.1 and the amplitude $T_{Vd \rightarrow pn}(s, u)$ to the contribution of the lower diagrams in the figure. Near threshold, where the cross section is isotropic we have

$$\overline{|T_{Vd \rightarrow pn}(s, t) + T_{Vd \rightarrow pn}(s, u)|^2} = 4 \overline{|T_{Vd \rightarrow pn}(s, t)|^2} \quad (14)$$

The differential cross section of the reaction

$$pn \rightarrow dV \quad (15)$$

can be expressed through $d\sigma/dt$ from Eq.(13) as follows

$$\frac{d\sigma_{pn \rightarrow dV}(s, t)}{dt} = \frac{9}{4} \left(\frac{p_V^{\text{cm}}}{p_p^{\text{cm}}} \right)^2 \frac{d\sigma_{Vd \rightarrow pn}(s, t)}{dt} \quad (16)$$

The cross sections of the reactions $pn \rightarrow d\phi$ and $pn \rightarrow d\omega$ are rather sensitive to the value of the cut-off parameter Λ . We take it in the interval $\Lambda = 1.0 - 1.2$ GeV. The cross section of the reaction $pn \rightarrow d\omega$ is rather big and at $T_p = 2.1$ GeV ($k_{\omega}^{\text{cm}}(s_1) \simeq 220$ MeV/c for the reaction $\pi^- p \rightarrow n\omega$) is in the range $34 - 60 \mu\text{b}$. The cross section for ϕ production is significantly smaller. It is in the range $0.16 - 0.33 \mu\text{b}$ at $T_{\text{lab}} = 2.8$ GeV ($k_{\phi}^{\text{cm}}(s_1) \simeq 220$ MeV/c for the reaction $\pi^- p \rightarrow n\phi$). Note that the maximum energy which can be reached at COSY-Jülich is 2.688 GeV.

It is interesting to compare the cross sections of the reactions $pn \rightarrow d\omega$ and $pp \rightarrow pp\omega$ close to threshold. The last one was measured by the SPES3 Collaboration at SATURNE (Saclay) at $T_{\text{lab}} = 1905 - 1935$ MeV [15] and analyzed within the framework of the meson-exchange model in Ref.[17]. Adjusting the cut-off parameter Λ_N of the form factor to the data the authors of Ref.[17] calculated the cross section of the reaction $pp \rightarrow pp\omega$ for proton incident energies up to 2.2 GeV. This model predicts a cross section of about $2 - 3 \mu\text{b}$ at 2.0 GeV. This is a factor $10 - 30$ smaller than the cross section of the reaction $pn \rightarrow d\omega$ predicted by the two-step model. A similar situation happens in the case of η -production near threshold where the cross section of the reaction

$pn \rightarrow d\eta$ is also much higher than the cross section of the reaction $pp \rightarrow pp\eta$ (see e.g. papers [26–28] and references therein). This is the consequence of two factors: i) the dominance of the isovector meson exchange mechanism which gives approximately a factor 6 in favour of the $pn \rightarrow pn\eta$ cross section as compared to $pp \rightarrow pp\eta$; ii) the influence of phase space close to threshold which suppresses the three-body final state as compared with the two-body state. The value of the suppression depends on the excess energy $Q = \sqrt{s} - \sqrt{s_0}$, where $\sqrt{s_0}$ is the CM-threshold energy (see Ref.[28]). At $Q = 20 - 30$ MeV it might be a factor up to 3 – 5. Another factor which enhances the cross section of the reaction $pn \rightarrow dV$ near threshold in our model is the constructive interference of the amplitudes $A(s, t)$ and $A(s, u)$. Very close to threshold where the cross section is isotropic and the interference of those amplitudes is complete it gives an enhancement factor of 4.

Let us note that our results for the $pn \rightarrow dV$ cross section are rather close to the prediction of the Rossendorf collision model $\sim 50 \mu\text{b}$ at 2.0 GeV [29] as well as to the estimate made by Wilkin ($\sim 30 \mu\text{b}$ at 2.0 GeV [30]).

3 The quark-gluon string model

The values of the cross sections presented in the previous section are only valid near threshold where they are proportional to k_{cm}^2 and the differential cross sections are isotropic. In order to describe the angular and energy dependence above threshold we use the quark-gluon string model (QGSM) developed by Kaidalov in [19]. For a sufficiently high energy \sqrt{s} and not very high t ($t \leq 12 \text{ GeV}^2$) the amplitude of the reaction $pn \rightarrow dV$ is dominated by the exchange of three valence quarks in the t -channel with any number of gluons exchanged between them (see Fig.2). The diagrams of Fig.2 a) and b) describe the exchange of three valence quarks in t - and u -channels, respectively. The important question is whether we can apply the QGSM at incident momenta of about 1 GeV/c.

The QGSM is based on two ingredients: i) the topological expansion in QCD and ii) the space-time picture of the interactions between hadrons, which takes into account the confinement of quarks. The $1/N_c$ expansion in QCD (where N_c is the number of colors) was proposed by 't Hooft [31]. The behavior of different quark-gluon graphs according to their topology was analyzed by Rossi and Veneziano [32]. In the large N_c limit the planar quark-gluon graphs are dominant. The QGSM proposed by Kaidalov [19] is based on the $1/N_f$ expansion with $N_c \sim N_f$ (where N_f is the number of flavours). At sufficiently large N_f the simplest planar quark-gluon graphs give dominant contribution into the amplitudes of binary hadronic reactions. For the amplitudes with definite quantum numbers in the t -channel, the parameter of expansion is

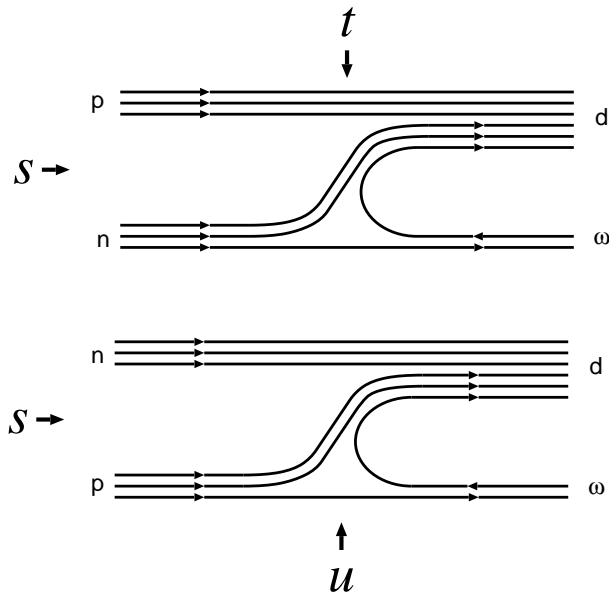


Fig. 2. Diagrams describing three valence quark exchanges in t - and u -channels.

$1/N_f^2 \sim 1/10$. In the space-time representation those graphs correspond to the formation and break-up of a quark-gluon string in the intermediate state. The quark-gluon string is identified with the corresponding Regge trajectory (in case of Fig.2 we have in the intermediate state the string with a quark and a diquark at the ends which corresponds to the nucleon Regge trajectory). Therefore, the QGSM can be considered as a microscopic model of the Regge phenomenology and can be used for calculations of different parameters which were treated before only on phenomenological level. In the QGSM each graph can be classified according to its topology and the amplitude corresponding to this graph can be considered as analytic function of s and t .

As it was shown by Kaidalov [19] the QGSM describes rather well the experimental data on the exclusive and inclusive hadronic reactions at high energy. Moreover due to the duality property of scattering amplitudes [32] this approach can also be applied in the intermediate energy region (see Ref.[33]), especially for reactions with no resonances in the direct channel. In fact this model was successfully applied to the description of the reactions $pp \rightarrow d\pi^+$, $\bar{p}d \rightarrow MN$ and $\gamma d \rightarrow pn$ at intermediate energies where the diagrams with three valence quark exchanges in the t -channel were found to be dominant (see [33–35]). So we expect that the QGSM will also give a reasonable description of reaction (2).

First of all we have to fix the spin structure of the $pn \rightarrow dV$ amplitude. We assume that it is equal to the one predicted by the two-step model (see Eq.(8)). Then the amplitude corresponding to the graph of Fig.2 (upper) can be written as

$$T_{pn \rightarrow dV}(s, t) = \varphi^{T^*}(\vec{n})(-i\sigma_y) \vec{\sigma} \cdot \vec{\epsilon}^{(d)} \vec{\sigma} \cdot \vec{\epsilon}^{(V)} \vec{\sigma} \cdot \hat{\vec{p}} \varphi(\vec{p}) \cdot A(s, t), \quad (17)$$

where \vec{p} and \vec{n} are the proton and neutron momenta respectively, $\hat{\vec{p}}$ is the unit vector directed along \vec{p} and $T(s, t)$ is the invariant amplitude, which corresponds to the nucleon Regge-trajectory

$$A(s, t) = F(t) \left(\frac{s}{s_0}\right)^{\alpha_{N(t)}} \exp\left[-i \frac{\pi}{2} \left(\alpha_{N(t)} - \frac{1}{2}\right)\right]. \quad (18)$$

Here $\alpha_{N(t)}$ is the trajectory of the nucleon Regge pole and $s_0 = m_d^2$. According to the data on πN backward scattering [36] it has some nonlinearity:

$$\alpha_{N(t)} = \alpha_{N(0)} + \alpha'_{N(0)} t + \frac{1}{2} \alpha''_{N(0)} t^2 \exp(-\beta t^2) \quad (19)$$

where $\alpha_{N(0)} = -0.5$, $\alpha'_{N(0)} = 0.9 \text{ GeV}^{-2}$ are the intercept and slope of the Regge trajectory, $\alpha''_{N(0)} = 0.4 \text{ GeV}^{-4}$ and $\beta = 0.03 \text{ GeV}^{-4}$. The exponential term in (19) is introduced to prevent the fast grow of the amplitude with s at large t which would be in contradiction with unitarity. The small value of β is chosen in order not to destroy the parameterization of $\alpha(t)$ at $-t \leq 1.6 \text{ GeV}^2$ found in [36].

The dependence of the residue $F(t)$ on t can be taken from [33,34]

$$F(t) = B \left[\frac{1}{m^2 - t} \exp(R_1^2 t) + C \exp(R_2^2 t) \right], \quad (20)$$

where the first term in the square brackets contains the nucleon pole and the second term contains also the contribution of nonnucleonic degrees of freedom in a deuteron. The parameters of the residue (except the overall normalization factor B) we take the same as in [33], which were found by fitting data on the reaction $pp \rightarrow \pi^+ d$ [37] at $-t \leq 1.6 \text{ GeV}^2$:

$$C = 0.7 \text{ GeV}^{-2}, R_1^2 = 3 \text{ GeV}^{-2} \text{ and } R_2^2 = -0.1 \text{ GeV}^{-2}. \quad (21)$$

Therefore, in our case we have only one free parameter B , which we define normalizing the differential cross section predicted by the QGSM

$$\frac{d\sigma_{pn \rightarrow dV}}{dt} = \frac{1}{64 \pi s} \frac{1}{(p_p^{\text{cm}})^2} \overline{|T_{pn \rightarrow dV}(s, t) + T_{pn \rightarrow dV}(s, u)|^2} \quad (22)$$

to the calculated one within the two-step model. As the normalization point we take $T_p = 2.1$ GeV for ω production and 2.8 GeV for ϕ production.

In Fig.3 we present the angular distributions for the reaction $pn \rightarrow d\omega$ at 2.0 and 2.6 GeV and for $pn \rightarrow d\phi$ at 2.6 and 2.688 GeV.

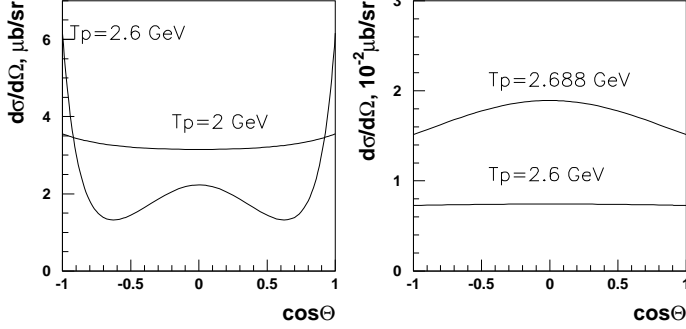


Fig. 3. Differential cross sections of the reactions $pn \rightarrow d\omega$ and $pn \rightarrow d\phi$.

We see that the angular distribution for ω production is almost isotropic at 2.0 GeV, which demonstrates the dominance of the S wave at least up to $p_\omega^{\text{cm}} = 0.207$ GeV/c. At 2.6 GeV, when many partial waves contribute, it has very sharp forward and backward peaks. The angular distribution of ϕ production is completely isotropic at 2.6 GeV ($p_\phi^{\text{cm}} = 0.07$ GeV/c); it becomes slightly non isotropic at 2.688 GeV ($p_\phi^{\text{cm}} = 0.206$ GeV/c) with an excess of about 20% at 90° as compared to the forward and backward angles. It can be concluded from Fig.3 that in both reactions the S wave dominates up to $p_V^{\text{cm}} \simeq 0.2$ GeV/c.

The energy dependence of the total cross sections of the reactions $pn \rightarrow d\omega$ and $pn \rightarrow d\phi$ is presented in in Fig.4. The upper and lower curves correspond to $\Lambda = 1.2$ and 1.0 GeV respectively. Rising above the threshold the cross sections of both reactions reach the maxima and then decrease following the power law $(s/s_0)^{2\alpha(0)-2}$. The maximum of the ω -production cross section is at incident energies covered by COSY. The maximum of the cross section for ϕ production is very close to the maximal energy which can be reached at COSY.

In Fig.5 we present the differential cross sections of the reactions $pn \rightarrow d\omega$ and $pn \rightarrow d\phi$ as functions of t at higher energies up to $T_p = 3.8$ GeV. For ω production the forward and backward peaks at 2.6, 3.2 and 3.8 GeV can clearly be seen. For ϕ production they are also rather well developed at 3.2 and 3.8 GeV. In the middle of all the curves there is a structure due to the interference of the diagrams corresponding to the t channel and u channel exchanges (see Fig.2).

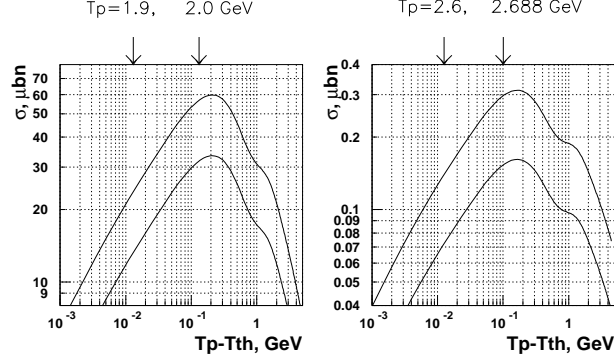


Fig. 4. Energy dependence of the cross sections for the reactions $pn \rightarrow d\omega$ and $pn \rightarrow d\phi$. The upper and lower curves are calculated for $\Lambda = 1.2$ and 1.0 GeV, respectively.

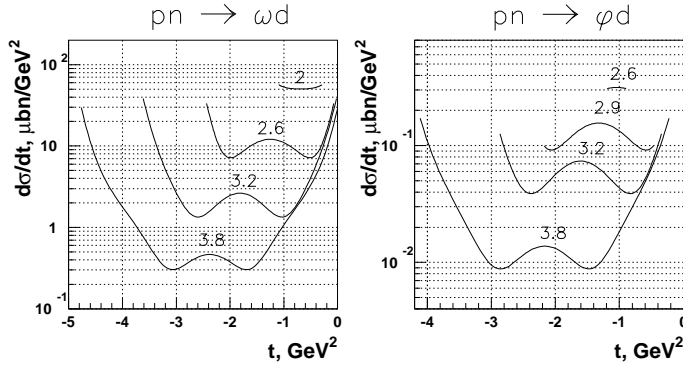


Fig. 5. Differential cross sections of the reactions $pn \rightarrow d\omega$ and $pn \rightarrow d\phi$ as functions of t at energies up to $T_p = 3.8$ GeV.

Let us now construct the ratio of the differential cross sections

$$R_0(s, t) = \frac{d\sigma(pn \rightarrow d\phi)/dt}{d\sigma(pn \rightarrow d\omega)/dt}. \quad (23)$$

In the region where the t -channel exchange is dominant and the u -channel exchange can be neglected, the ratio $R_0(s, t)$ would be independent of s and t in our model. The same will happen in the region where the u -channel exchange is dominant. However, if both exchanges are significant the value of $R_0(s, t)$ will depend on s and t and this dependence will be strongest at $\theta_{\text{cm}} = 90^\circ$, where the interference is maximal.

Certainly, it is more convenient to consider the ratio $R_0(s, t)$ in those kinematical regions where it is a rather smooth function of the kinematical variables. From this point of view kinematical regions where only one mechanism is dominant are preferable. To illustrate this point we present in Fig.6 the differential cross sections of the reactions $pn \rightarrow d\omega$ and $pn \rightarrow d\phi$ at $\theta_{\text{cm}} = 0^\circ$ as functions of s . We see that at $s \leq 10$ GeV² the behavior of the differential cross sections (as well as their ratio) is oscillating which is caused by the strong

interference of the t and u channel exchanges. However above $s = 12 \text{ GeV}^2$ both cross sections decrease with s like s^{-3} and their ratio $R_0(s, \theta_{\text{cm}} = 0^\circ)$ becomes independent of s and converges to a value of 10×10^{-3} .

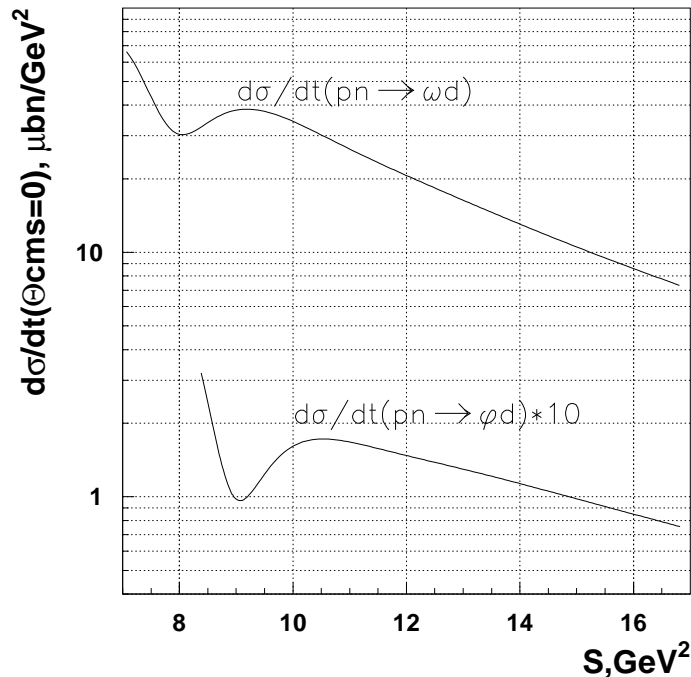


Fig. 6. Differential cross sections of the reactions $pn \rightarrow d\omega$ and $pn \rightarrow d\phi$ at $\theta_{\text{cms}} = 0^\circ$ as functions of s .

Another possibility is to compare the S -wave amplitudes of the reactions $pn \rightarrow d\omega$ and $pn \rightarrow d\phi$. Near the corresponding thresholds where the S wave is dominant the t and u channel exchange amplitudes are equal and do not depend on the scattering angle. In Fig.7 we show the invariant amplitudes squared $|A_\omega|^2$ and $|A_\phi|^2$ for both reactions calculated using our model. Their ratio is equal to 6×10^{-3} at $p_V^{\text{cm}} = 0.2 \text{ GeV}/c$. Having in mind that each cross section has an uncertainty of about 30%, the ratio R can be written as:

$$R = |A_\phi|^2 / |A_\omega|^2 = (4 - 8) \times 10^{-3}. \quad (24)$$

Thus the model based on the dominance of hadronic intermediate states predicts a rather small ratio of the S -wave amplitudes for ϕ and ω production.

Another estimate of R can be found if we assume the line-reverse invariance of the amplitudes, which correspond to the diagrams presented in Fig.2. In this case we have

$$\begin{aligned} \overline{|T_{pn \rightarrow dV}^{\text{LRI}}(s, t)|^2} &= \overline{|T_{pn \rightarrow dV}^{\text{LRI}}(s, t) + T_{pn \rightarrow dV}^{\text{LRI}}(s, u)|^2} \\ &= \overline{|T_{pd \rightarrow nV}(s, t) + T_{pd \rightarrow nV}(s, u)|^2} \end{aligned} \quad (25)$$

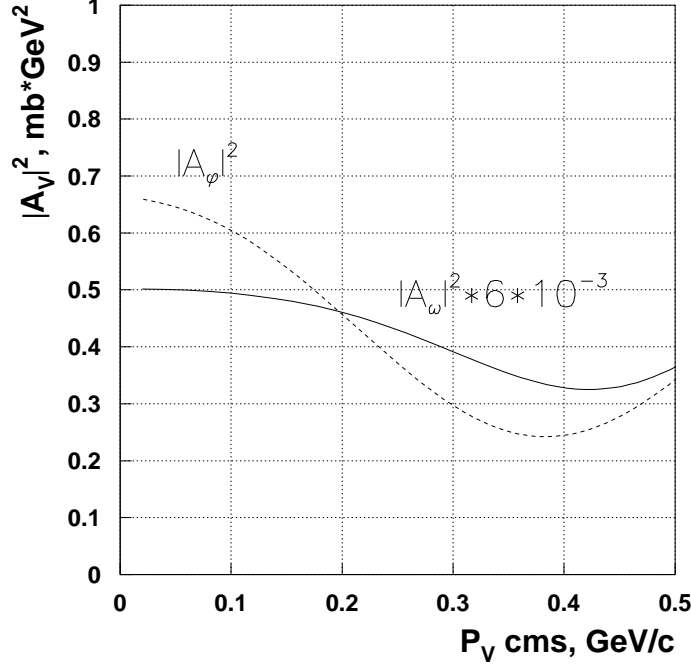


Fig. 7. Invariant amplitudes squared for the reactions $pn \rightarrow d\omega$ and $pn \rightarrow d\phi$ as functions of the final momentum in the CM system.

and can define the ratio

$$R_{\text{LRI}} = |T_{pn \rightarrow d\phi}^{\text{LRI}}|^2 / |T_{pn \rightarrow d\omega}^{\text{LRI}}|^2 = |T_{\bar{p}d \rightarrow n\phi}^{\text{LRI}}|^2 / |T_{\bar{p}d \rightarrow n\omega}^{\text{LRI}}|^2. \quad (26)$$

Adopting the result of the OBELIX collaboration $Y(\bar{p}d \rightarrow n\phi)/Y(\bar{p}d \rightarrow n\omega) = (230 \pm 60) \times 10^{-3}$ we get

$$\begin{aligned} R_{\text{LRI}} &= |T_{\bar{p}d \rightarrow n\phi}^{\text{LRI}}|^2 / |T_{\bar{p}d \rightarrow n\omega}^{\text{LRI}}|^2 \\ &\simeq (p_{\text{cm}}^\omega / p_{\text{cm}}^\phi) (Y(\bar{p}d \rightarrow n\phi) / Y(\bar{p}d \rightarrow n\omega)) \simeq (250 \pm 60) \times 10^{-3}, \end{aligned} \quad (27)$$

which is larger by more than an order of magnitude than that from the two-step model for the reaction $pn \rightarrow dV$.

As the two-step model describes very well the Pontecorvo reactions we conclude that LRI (and QGSM) is violated in the case of the reactions $pn \rightarrow d\omega$ and $\bar{p}d \rightarrow n\omega$ near threshold. Let us discuss possible reasons of this violation.

According to [33] the line reverse invariance (LRI) works fairly well in the case of the reactions $pp \rightarrow d\pi^+$ and $\bar{p}d \rightarrow p\pi^-$. However, there are two regions where the experimental data on the $pp \rightarrow d\pi^+$ total cross section are noticeably larger than the theoretical expectations:

i) at $\sqrt{s} = 2.17$ GeV there is a strong contribution from intermediate production of the Δ -isobar;

ii) around 2.9 GeV there is a resonance-like structure in the cross section which might be a signal of a broad dibaryon (see e.g. [38] and references therein).

Using experimental BR's for the reactions $\bar{p}d \rightarrow n\omega$ and $\bar{p}d \rightarrow n\phi$ at rest (see Table 1) we can fix the values of the parameter B in Eq.(20) and calculate the cross sections of the line-reversed reactions $pn \rightarrow d\omega$ and $pn \rightarrow d\phi$. In the case of the reaction $pn \rightarrow d\omega$ we found $\sigma_{pn \rightarrow d\omega}^{\text{LRI}} = 4.3 \mu\text{b}$ at $T_p = 2.0$ GeV, which is about 7 – 12 times smaller than the cross section predicted by the two-step model.

This strong violation of LRI in the case of the reactions $pn \rightarrow d\omega$ and $\bar{p}d \rightarrow \omega n$ might indicate that there is a strong resonance effect in the ωN channel close to threshold. A possibility that there might be a resonance in the reaction $\pi^- p \rightarrow \omega n$ near the threshold was discussed earlier in [25]. It is also known that in the ρN channel there are many resonances, which contribute essentially to the cross sections of the reactions $\pi N \rightarrow \rho n$ [39] and $\rho N \rightarrow \rho N$ [40] close to threshold. The baryon resonances with isospin $I = 1/2$ can also couple to the ωN channel.

In the case of the reaction $pn \rightarrow d\phi$ we have: $\sigma_{pn \rightarrow d\phi}^{\text{LRI}} = 0.22 \mu\text{b}$ at $T_p = 2.7$ GeV, which is in perfect agreement with the prediction of the two-step model. Therefore, in the case of ϕ production LRI is not violated and we may think that this a hint that resonance effects in the amplitude $\pi N \rightarrow N\phi$ near threshold are absent. So the measurements of ω and ϕ production in pp , and pd collisions near the threshold are also interesting from the point of view of searching for resonances in the $\omega(\phi)N$ channel.

4 Conclusions

Using the two-step model which is described by triangle graphs with π -mesons in the intermediate state we calculated the cross sections of the reactions $pn \rightarrow dV$, where $V = \omega$ or ϕ , close to threshold and found a ratio of the S -wave amplitudes squared to be $R = |A_\phi|^2/|A_\omega|^2 = (4-8) \times 10^{-3}$. If a significant enhancement of $R(\phi/\omega)$ over the value predicted by the two-step model will be found in future experimental data, it might be interpreted as a possible contribution of the intrinsic $s\bar{s}$ component in the nucleon wave function.

The two-step model yields a cross section for the reaction $pn \rightarrow d\omega$ which is 7 – 12 times larger than it is predicted with the help of the LRI assumption from the experimental BR for the reaction $\bar{p}d \rightarrow \omega n$. We interpret this result as an evidence of a strong resonance effect in the ωN channel close to threshold. In the case of ϕ production near threshold in the reaction $pn \rightarrow d\phi$ the cross section is in perfect agreement with the prediction of LRI.

We also analyzed the reaction $pn \rightarrow dV$ at higher energies within the framework of the QGSM, where the amplitude can be described by contributions of three valence-quark exchange in the t and u channels. We calculated the differential cross sections of the reactions $pn \rightarrow d\omega$, $pn \rightarrow d\phi$ and the ratio of the ϕ/ω yields in a wide energy interval as functions of t . Essential interference between t - and u -channel contributions was found at $s \leq 12 \text{ GeV}^2$, where at small t the ϕ/ω ratio exhibits irregular behavior as a function of s .

Acknowledgements

We are grateful to W. Cassing, M.G. Sapozhnikov and C. Wilkin for useful discussions.

References

- [1] H. J. Lipkin, *Phys. Lett. B* **60** (1976) 371.
- [2] J. Ellis, E. Gabathuler and M. Karliner, *Phys. Lett. B* **217** (1989) 173.
- [3] J. Ellis, M. Karliner, D. E. Kharzeev and M. G. Sapozhnikov, *Phys. Lett. B* **353** (1995) 319.
- [4] S. Okubo, *Phys. Lett. B* **5** (1963) 165;
G. Zweig, *CERN Report* **8419/TH 412** (1964);
I. Iizuka, *Prog. Theor. Phys. Suppl.* **37-38** (1966) 21.
- [5] M. P. Locher, Y. Lu and B. S. Zou, *Z. Phys. A* **347** (1994) 281.
- [6] D. Buzatu and F. Lev, *Phys. Lett. B* **329** (1994) 143.
- [7] R. L. Jaffe, *Phys. Rev. Lett. B* **229** (1989) 275.
- [8] U.-G. Meissner, V. Mull, J. Speth and J. W. Van Orden, *Preprint KFA-IKP(TH)-1997-01*, Forschungszentrum Jülich (1997).
- [9] L. A. Kondratyuk and M. G. Sapozhnikov, *Phys. Lett. B* **220** (1989) 333;
L. A. Kondratyuk and M. G. Sapozhnikov, *Few Body Systems*, **Suppl.5** (1992) 201.
- [10] L. A. Kondratyuk, M. P. Bussa, Y. S. Golubeva, M. G. Sapozhnikov and L. Valacca, *Yad. Fiz.* **61** (1998), to be published.
- [11] R. Wurzinger et al., *Phys. Rev. C* **51** (1995) R443.
- [12] R. Wurzinger et al., *Phys. Lett. B* **374** (1996) 283.
- [13] G. Fäldt and C. Wilkin, *Nucl. Phys. A* **587** (1995) 769.

- [14] L. A. Kondratyuk and Y. N. Uzikov, *Yad. Fiz.* **60** (1997) 542.
- [15] Collaboration CRN Strasburg, IPN Orsay, LNS Saclay, in *Nouvelles de Saturne* no.19, Saclay (1995) 51.
- [16] A. Brenschede, *Ph.D. Thesis*, Universität Giessen (1997).
- [17] K. Nakayama, A. Szczurek, C. Hanhart, J. Haidenbauer, and J. Speth, *Phys. Rev. C* **57** (1998) 1580.
- [18] OBELIX collaboration, *Yad. Fiz.* **59** (1996) 1511.
- [19] A. B. Kaidalov, *Z. Phys. C* **12** (1982) 63.
- [20] OBELIX Collaboration, *Nuovo Cimento A* **107** (1994) 2837.
- [21] CRYSTAL BARREL Collaboration, *Z.Phys. A* **351** (1995) 325.
- [22] M. Lacombe et al., *Phys. Lett. B* **101** (1981) 139.
- [23] J. Cougnon, P. Denev and J. Vandermeulen, *Phys. Rev. C* **41** (1990) 1701.
- [24] A. Sibirtsev, *Nucl. Phys. A* **604** (1996) 455.
- [25] D. M. Binnie et al., *Phys. Rev. D* **8** (1973) 2789.
- [26] F. Plouin, P. Fleury and C. Wilkin, *Phys. Rev. Lett.* **65** (1990) 690.
- [27] E. Chiavassa et al., *Phys. Lett. B* **337** (1994) 192.
- [28] G. Fäldt and C. Wilkin, *Nucl. Phys. A* **604** (1996) 441.
- [29] H. Müller, *IKP Annual Report 1997, Berichte des Forschungszentrums Jülich* **3505** (1998) 77.
- [30] C. Wilkin, *private communication*.
- [31] G. 't Hooft, *Nucl. Phys. B* **72** (1974) 461.
- [32] G. C. Rossi and G. Veneziano, *Nucl. Phys. B* **123** (1977) 507.
- [33] A. B. Kaidalov, *Sov. J. Nucl. Phys.* **53** (1991) 872.
- [34] C. Guaraldo, A. B. Kaidalov, L. A. Kondratyuk and Ye.S. Golubeva, *Yad. Fiz.* **59** (1996) 1832.
- [35] L. A. Kondratyuk, E. De Sanctis, P. Rossi et al., *Phys. Rev. C* **48** (1993) 2491.
- [36] V. A. Lyubimov, *Sov. Phys. Uspekhi* **20** (1977) 691.
- [37] J. V. Allaby et al., *Phys. Lett. B* **29** (1969) 139;
U. Amaldi et al., *Lett. Nuovo Cimento* **4** (1972) 121;
H. L. Anderson et al., *Phys. Rev. D* **3** (1971) 1536; **9** (1973) 580.
- [38] L. A. Kondratyuk and A. V. Vasilets, *Nuovo Cim. A* **102** (1989) 25.
- [39] Particle Data Group, *Phys. Rev. D* **54** (1996).

- [40] L. A. Kondratyuk, A. Sibirtsev, W. Cassing, Ye. S. Golubeva and M. Effenberger, "Rho meson properties at finite nuclear density", *Preprint UGI-97-4*, Giessen University, January 1998; nucl-th/9801055; *Phys.Rev. C* to be published.